Chesi Alessandra (Orcid ID: 0000-0002-0954-7446)
Hankenson Kurt (Orcid ID: 0000-0003-1432-747X)
Grant Struan (Orcid ID: 0000-0003-2025-5302)

CRISPR-Cas9 mediated genome editing confirms *EPDR1* as an e

GWAS-implicated '*STARD3NL*' locus

James A. Pippin B.A.[1], Alessandra Chesi Ph.D.[1], Yadav Wagley Ph.D

Matthew C. Pahl Ph.D[1], Kenyaita M. Hodge B.A.[6], Matthew E. Johnso

Ph.D.[1,3], Kurt D. Hankenson, D.V.M., Ph.D.[2] and Struan F.A. Grant Ph

[1]Center for Spatial and Functional Genomics, Children's Hospital of P

United States, [2]Department of Orthopedic Surgery, University of Mich

Arbor, United States, [3]Department of Pathology and Laboratory Medic

Pennsylvania Perelman School of Medicine, Philadelphia, United Stat

Pediatrics, University of Pennsylvania Perelman School of Medicine,

States, [5]Divisions of Genetics and Endocrinology, Children's Hospital

Philadelphia, United States, [6]Genetics and Molecular Biology Gradua

Graduate School, Emory University, Atlanta, United States

ABSTRACT

Genome wide association studies (GWAS) have discovered genetic s
with bone mineral density (BMD), but typically not the precise localiza
intersecting genome-wide promoter-focused Capture C and ATAC-se
human mesenchymal progenitor cell (hMSC)-derived osteoblasts, we
consistent contacts between the *EPDR1* promoter and multiple BMD-
causal variants at the '*STARD3NL*' locus. We further showed that RN
expression in hMSC-derived osteoblasts led to inhibition of osteoblas
characterize the physical connection between these putative non-cod
locus and the *EPDR1* gene, we conducted CRISPR-Cas9 genome ed
across the single open chromatin region harboring candidates for the
rs1524068, rs6975644 and rs940347, all in close proximity to each ot
immunoblotting revealed dramatic and consistent downregulation of *E*
edited differentiated osteoblast cells. Consistent with *EPDR1* express
phosphatase staining was also markedly reduced in the edited differe
CRISPR-Cas9 genome editing in the hFOB1.19 cell model supports c
where this regulatory region harboring GWAS-implicated variation op

INTRODUCTION

Bone mineral density (BMD) is a key clinical measure used to ass
of the age-related disease, osteoporosis[1]. Low BMD is associated w
including low trauma events in osteoporosis patients[2]. BMD is highly
wide-association studies (GWAS) having already identified hundreds
disease risk across both adults[3] [1] and children[4] [5]. While some prog
recent years with development of new methods to treat osteoporosis[
investigation of BMD loci identified by GWAS should reveal target ge
potentially novel therapeutic avenues for prevention and treatment of

Often the sentinel single nucleotide polymorphism (SNP) identifie
causal SNP but instead a proxy SNP in close linkage disequilibrium t
causal SNP[8]. We recently published a high-resolution variant-to-ge
BMD GWAS loci in a disease-relevant cellular context: human mesen
osteoblasts (hMSCs)[9]. We placed two constraints on our data derive
differentiated into osteoblasts, first that SNPs in strong linkage disequ
GWAS sentinel variant must be accessible as determined by Assay fo
Chromatin using sequencing (ATAC-seq), and second that these acc
be in direct physical contact with an accessible promoter as determin

In that initial study, *EPDR1* (encoding ependymin related protein 1
implicated genes we examined and demonstrated an influence on bot
adipogenesis. The *EPDR1* gene resides at the '*STARD3NL'* locus (se
minor allele frequency: ~35%), and down-regulation of its expression
(RNAi) in BMP2-induced hMSC-derived osteoblasts revealed a decre
phosphatase (ALP) and Alizarin red S (ARS) staining, two fundament
osteoblastogenesis[9]. Further analysis revealed a reciprocal role for *E*
differentiation of the same hMSCs. Silencing of *EPDR1* increased the
during adipogenic differentiation of hMSCs, which was accompanied
C/EBP alpha and *PPAR* gamma, two key adipogenic transcription fac

While our RNAi approach provided valuable insight into the poten
osteoblast differentiation, it did not prove a direct regulatory connectio
implicated proxy SNPs and this putative effector gene. To determine
associated tight proxy SNP cluster resides in a cis-regulatory element
gene, we sought to delete the open chromatin region (OCR) harboring
SNPs to the sentinel (which are in strong linkage disequilibrium (LD) a
using clustered regularly interspaced short palindromic repeat Cas9 e
Cas9) mediated gene editing (**Figure 1**). We have successfully applie

approach in primary hMSCs, given their lack of proliferation ability. He
alternative cell model, an immortalized human fetal osteoblastic cell li
characterization of regulatory regions for human osteoblastogenesis.
easily passaged and expanded, a key requirement for CRISPR target
temperature-sensitive mutant, tsA58, of the SV40 large T antigen that
edited cells to proliferate under permissive conditions (33.5°C), and to
into osteoblasts at a higher temperature (39.5°C) [11]. This allowed us
variant-to-gene contact between the proxy SNPs and the *EPDR1* gen
'*STARD3NL'* locus at various stages of differentiation.

MATERIALS AND METHODS

Cell Culture

hFOB1.19 and 293T cells were cultured in the recommended med
standard culture conditions at 33.5°C and 37°C respectively. Different
into mature osteoblasts was accomplished by growing the cells at 39.
experiments. (see supplemental **Detailed Materials and Methods** fo

RNAi treatment

Cells were seeded in 12-well plates and RNAi transfections were
sets of 4 ON-TARGETplus RNAis (see **Supplemental, Table 1**) acco
instructions. Twenty-four hours later, media was replaced with fresh g
designated for differentiation into mature osteoblasts were moved to 3
and cells were allowed to grow until assayed for ALP staining after 5
Detailed Materials and Methods for details).

CRISPR Constructs, Lentivirus Production, hFOB1.19 Infection

The synthesized sgRNAs were cloned into the LentiCRISPRv2-m
modified Golden Gate assembly method [12] [13] [14] (see **Supplementa**

Freshly thawed hFOB1.19 cells were plated and allowed to adher
was replaced with fresh growth media, filtered lentivirus, and Polybre
infection. Media was replaced after 72 hrs. and cells were checked fo
(see **Supplemental Figure 1**). Lentiviral transduction efficiency was e
of both bright field live and mCherry positive cells. Cells were split pos
stocks and experimental plates to allow for assaying the cells at an ea
to the original cells as possible. (see supplemental **Detailed Material**
details).

Multiplex Sequencing

Genomic DNA from CRISPR-edited plates was extracted, quantita
proxy SNP target region was amplified by PCR (see **Supplemental F**
Supplemental Table 1) in three concurrent reactions. The final PCR
sequencing primers approximately 50bp upstream of each CRISPR c
coverage for all possible CRISPR-cas9 splicing sites. To eliminate pri
the PCR reactions was followed by a purification step. Libraries were
checked on a Bioanalyzer 2100 (Agilent) for quality before being pool
were sequenced on the MiSeq System (Illumina).

Alkaline Phosphatase Assay

ALP staining was assessed as described in previous studies with
CRISPR-edited hFOB1.19 cells were seeded in two 12-well plates all
The following day, one plate was moved to 39.5°C and allowed to diff
the other remained at 33.5°C. On the day of the ALP assay, fresh fixa
were prepared, media was removed, and cells were washed with DPB
plate, washed with ultrapure water, and staining solution was applied
development of color. Once staining was complete, cells were washe
allowed to air dry. Plates were photographed and images were conve
quantification using Image J software as previously described[9]. (see
Materials and Methods for details).

Reverse Transcription-quantitative Polymerase Chain Reaction (

RNA was isolated from CRISPR-edited hFOB1.19 cells after 7 da
(39.5°C). RNA was subsequently purified, converted into cDNA, and s
gene specific primers (see **Supplemental Table 1**). Results were exp
GAPDH and fold change calculated using Cq (ΔR) values and the co

with EPDR1 antibody (Abcam, ab197932) and α-Tubulin antibody (Sa
Inc., sc-58666). On the following day, membranes were washed, incu
Peroxidase (HPR) linked secondary antibodies (Santa Cruz Biotechn
developed with chemiluminescent substrate and visualized using the
System (Thermo). Quantification of Western immunoblotting bands w
build-in software on the iBright system. (see supplemental **Detailed M**
details).

RESULTS

RNAi knock-down of *EPDR1* gene expression and alkaline phosp differentiated hFOB1.19 Cells

To validate differentiated hFOB1.19 cells as a comparable model stem cell (hMSC)-derived osteoblasts for our line of investigation, we of *EPDR1* expression in hFOB1.19 cells. Our previous RNAi targeting derived osteoblasts resulted in lower levels of both alkaline phosphata Alizarin red S staining (ARS)[9]. ALP activity is necessary for hydroxya mineralization[16], while ARS stains for the deposition of calcium[17]. H cells undergo osteoblast differentiation, they do not produce an appre for detection by ARS[18]. Therefore, we elected to use ALP staining al differentiation. To confirm the same response as observed in hMSC-d carried out RNAi targeting of *EPDR1* expression in differentiated hFO was markedly increased during differentiation of hFOB1.19 cells, whil undifferentiated cells and in *EPDR1* RNAi treated cells under differen this reduction was more pronounced than our observations in hMSC-d (**Supplemental Figure 3A and 3B**). This confirmed that the hFOB1.1 cellular model to study preliminary osteoblast differentiation, and that

the '*STARD3NL*' locus, which are all in close proximity (rs1524068, rs
Given that the three proxy SNPs are harbored within a 204bp region a
each other with respect to LD, we designed a pooled set of three sgR
each side of the proxy SNP set to delete the entire region of open chr
Supplemental Figure 2). mCherry expression in CRISPR targeted ce
lentiviral transduction efficiency and averaged ~87% (see **Suppleme**
high efficiency allowed us to proceed without cell sorting; however, it
result of this approach, all subsequent results included at least 10% n

PCR and multiplexed sequencing validation of pooled CRISPR h

PCR primers flanking the targeted region were used to amplify ge
the CRISPR edited hFOB1.19 cells (see **Supplemental Figure 2** and
products were further selected for specificity with a nested set of PCR
from both wild type and CRISPR deletions fell within the predicted siz
Figure 5). The wild type product was 2,370 base pairs (bp) in size, wh
CRISPR-edited pooled cells ranged from 595bp to 1,739bp (PCR ban
To further verify each CRISPR deletion, all PCR products were seque
next generation sequencing adapter primer strategy modified from pr

qPCR analysis of *EPDR1* RNA expression in pooled CRISPR hFO

Given that distal cis-regulatory elements generally regulate gene e
order to physically cooperate with the promoter and/or proximal upstre
hypothesized that contacts between the putative causal SNP region a
regulate *EPDR1* gene expression. To test this, we measured *EPDR1*
using gene specific primers (see **Supplemental Table 1**) on control (
LentiCRISPRv2-mCherry construct containing no sgRNA sequence) c
hFOB1.19 cells growing for five days under either permissive or differ
all samples were first normalized to *GAPDH* expression and then norm
empty vector control samples, a large increase in *EPDR1* mRNA was
differentiated control samples, but *EPDR1* mRNA levels remained sig
differentiated pooled CRISPR-edited samples (**Figure 3**). No differenc
expression was observed in the cells growing under undifferentiated c
Normalization of CRISPR samples to *GAPDH* for the corresponding p
controls, respectively, revealed levels of *EPDR1* mRNA in differentiat
hFOB1.19 cells were reduced 3- to 7-fold compared to controls and u
undifferentiated cells (**Supplemental Figure 6**). Taken together, this

immunoblot analysis. As shown in **Figure 4A**, EPDR1 protein expres
reduced in the pooled CRISPR-edited hFOB1.19 cells grown under di
but not in those grown under permissive conditions, which is consiste
observed for *EPDR1* mRNA levels. Quantification of both the upper b
(M) present across all samples showed ~70-90% decrease in EPDR1
normalized to Tubulin, but in the differentiated samples only. (**Figure**

Alkaline phosphatase activity in pooled CRISPR-edited hFOB1.19

Alkaline phosphatase activity is an important biomarker of osteobl
therefore we sought to confirm that this decrease in *EPDR1* expressio
differences in ALP activity in differentiated hFOB1.19 cells lacking the
causal SNP region. Pooled CRISPR-edited hFOB1.19 replicates were
permissive and differentiation conditions for five days. Plates were the
activity in the same manner used for RNAi treated cells. As shown in
induced ALP staining was reduced in CRISPR-edited hFOB1.19 cells
quantification of ALP staining revealed a 40-76% decrease in this stai
presume a portion of the staining in the CRISPR-edited cells is due to
cells (approximately 10%) in our pooled replicates. This decrease in A

DISCUSSION

In our previous study, we implicated a putative regulatory region h
three BMD GWAS proxy SNPs interacting with *EPDR1*, a gene not pr
involved in bone metabolism[9]. It should be noted that the previous st
genes implicated in osteoblastogenesis using this method and the sa
more generally applied to other GWAS studies and cell model system
sought to fully validate the regulatory connection between the SNP ha
'*STARD3NL*' locus and the implicated *EPDR1* gene. Deleting this reg
putative underlying causal SNP in hFOB1.19 cells by CRISPR-Cas9 p
for an *EPDR1* regulatory function of this region at both the RNA and p
interestingly, this regulation is cell differentiation state specific. The ne
Figure 1) was not detectable by qPCR and showed no significant cha
hFOB1.19 cells (data not shown). Thus, these studies also support ou
EPDR1 plays a role in osteoblastogenesis by validating the putative r
effect on ALP activity through CRISPR-based perturbation.

GWAS studies have proven very informative in identifying highly a
interest within the genome, but very often the identified SNP is not ca
effector gene still has to be elucidated. In addition, target validation fo

could play a direct transcriptional regulatory role. [22] EPDR1 is also kn
extracellular matrix proteins which are known to play a role in osteobl
Furthermore, EPDR1 peptides have been shown to play a role in tran
transcription factor involved in osteoblast differentiation through TGF-
vitamin D [25,26]; thus AP-1 transcriptional activity may reveal another r
setting, and therefore warrants follow-up efforts. These other studies s
represents an attractive novel target for bone metabolism. While EPD
impairs gene expression, elucidating the impact of reduced EPDR1 o
protein level will be essential.

While the present study confirms a regulatory role for the proxy SN
in *EPDR1* gene regulation, due to the tight proximity of the three BMD
SNPs, the identity of the exact causal variant remains unknown. Ident
SNP(s) involved will require more precise techniques than CRISPR-C
this region. Other sequence specific techniques like CRISPR inhibitio
CRISPR activation (CRISPRa) which have no endonuclease activity b
at the sgRNA guide position without modifying the genome or CRISP
synchronous programmable adenine and cytosine editor (SPACE) [24]
targeting of the individual alleles. Potential binding sites for transcripti

This work also builds on efforts by other groups to connect osteop
signals directly to the transcription of a distal gene, and thus downstre
While additional studies are needed to further explore the regulation o
'STARD3NL' locus and to understand its mechanistic function, our cu
points to *EPDR1* being involved in bone differentiation processes and
target for BMD-related osteoporosis studies.

ACKNOWLEDGMENTS

This research was funded by the Children's Hospital of Philadelphia a

HG010067, R01 AR066028 and R01 HD100406. Dr. Grant is funded

Endowed Chair for Diabetes Research.

DISCLOSURES

The authors report no conflicts of interest

REFERENCES

1. Morris JA, Kemp JP, Youlten SE, Laurent L, Logan JG, Cha
Forgetta V, Kleinman A, Mohanty ST, Sergio CM, Quinn J,
Luco A-L, Vijay J, Simon M-M, Pramatarova A, Medina-Gor
Ghirardello EJ, Butterfield NC, Curry KF, Leitch VD, Sparke
Mannan NS, Komla-Ebri DSK, Pollard AS, Dewhurst HF, Ha
23andMe Research Team, Adams DJ, Vaillancourt SM, Kap
Cooper C, Reeve J, Ntzani EE, Evangelou E, Ohlsson C, K
Kiel DP, Tobias JH, Gregson CL, Harvey NC, Grundberg E,
Lelliott CJ, Hinds DA, Ackert-Bicknell CL, Hsu Y-H, Mauran
Williams GR, Bassett JHD, Evans DM, Richards JB. An atla
osteoporosis in humans and mice. Nature Genetics. Nature
Feb;51(2):258–66.

2. Richards JB, Zheng H-F, Spector TD. Genetics of osteopor
association studies: advances and challenges. Nat. Rev. Ge
18;13(8):576–88.

3. Kemp JP, Morris JA, Medina-Gomez C, Forgetta V, Warring
Zheng J, Gregson CL, Grundberg E, Trajanoska K, Logan J
PC, Ghirardello EJ, Allen R, Leitch VD, Butterfield NC, Kom
Curry KF, White JK, Kussy F, Greenlaw KM, Xu C, Harvey
Greenwood CMT, Maurano MT, Kaptoge S, Rivadeneira F,
Ackert-Bicknell CL, Bassett JHD, Williams GR, Richards JB
of 153 new loci associated with heel bone mineral density a
of GPC6 in osteoporosis. Nature Genetics. 2017 Oct;49(10)

4. Chesi A, Mitchell JA, Kalkwarf HJ, Bradfield JP, Lappe JM,
McCormack SE, Gilsanz V, Oberfield SE, Hakonarson H, S
Zemel BS, Grant SF. A Genomewide Association Study Ide
Loci, at SPTB and IZUMO3, Influencing Pediatric Bone Min
Skeletal Sites. Journal of Bone and Mineral Research. 2017

5. Chesi A, Mitchell JA, molecular HKH, 2015. A trans-ethnic g
study identifies gender-specific loci influencing pediatric aBM

interactions implicate effector genes at GWAS loci for bone
Communications. Springer US; 2019 Mar 13;:1–11.

10. Xia Q, Chesi A, Manduchi E, Johnston BT, Lu S, Leonard M
EF, Huang P, Wells AD, Blobel GA, Johnson ME, Grant SF
presumed causal variant within TCF7L2 resides in an eleme
expression of ACSL5. Diabetologia. Springer Berlin Heidelb
Nov;59(11):2360–8.

11. Harris SA, Enger RJ, Riggs LB, Spelsberg TC. Developmen
conditionally immortalized human fetal osteoblastic cell line
Mineral Research. John Wiley & Sons, Ltd; 1995 Feb 1;10(2

12. Engler C, Kandzia R, Marillonnet S. A One Pot, One Step, P
with High Throughput Capability. El-Shemy HA, editor. PLo
Science; 2008 Nov 5;3(11):e3647–7.

13. Engler C, Gruetzner R, Kandzia R, Marillonnet S. Golden G
DNA Shuffling Method Based on Type IIs Restriction Enzym
PLoS ONE. Public Library of Science; 2009 May 14;4(5):e5

14. Engler C, Marillonnet S. Generation of Families of Construc
Gate Shuffling. In: Lu C, Browse J, Wallis JG, editors. cDNA
Applications. Totowa, NJ: Humana Press; 2011. pp. 167–81

15. Schmittgen TD, Livak KJ. Analyzing real-time PCR data by
method. Nat Protoc. Nature Publishing Group; 2008 Jun 1;3

16. Orimo H. The mechanism of mineralization and the role of a
health and disease. J Nippon Med Sch. The Medical Assoc
School; 2010 Feb;77(1):4–12.

17. Serguienko A, Wang MY, Myklebost O. Real-Time Vital Min
Quantification during In Vitro Osteoblast Differentiation. Bio
2018 May 30;:1–5.

18. Wanachewin O, Boonmaleerat K, Pothacharoen P, Reutrak

21. Nimmrich I, Erdmann S, Melchers U, Chtarbova S, Finke U, Oertel M, Hoffmann W, Müller O. The novel ependymin rela expressed in colorectal tumor cells. Cancer Lett. 2001 Apr 1

22. Deshmukh AS, Peijs L, Beaudry JL, Jespersen NZ, Nielsen Larsen TJ, Bayarri-Olmos R, Prabhakar BS, Helgstrand C, Kjaer A, Tang-Christensen M, Sanfridson A, Garred P, Priv Gerhart-Hines Z, Nielsen S, Drucker DJ, Mann M, Scheele Comparative Mapping of the Secretomes of Human Brown Reveals EPDR1 as a Novel Batokine. Cell Metabolism. Else 5;30(5):963–7.

23. Shashoua VE, Adams D, Boyer-Boiteau A. CMX-8933, a pe glycoprotein ependymin, promotes activation of AP-1 transc neuroblastoma and rat cortical cell cultures. Neurosci. Lett. 7.

24. Grünewald J, Zhou R, Lareau CA, Garcia SP, Iyer S, Miller Aryee MJ, Joung JK. A dual-deaminase CRISPR base edito adenine and cytosine editing. Nat. Biotechnol. Nature Publis 1;38(7):861–4.

25. Trzeciakiewicz A, Habauzit V, Horcajada M-N. When nutriti function: molecular mechanisms of polyphenols. Nutr. Res. Pennsylvania Libraries; 2009 Feb 26;22(1):68–81.

26. Chang J, Wang Z, Tang E, Fan Z, McCauley L, Franceschi PH, Wang C-Y. Inhibition of osteoblastic bone formation by Med. Nature Publishing Group; 2009 May 17;15(6):682–9.

27. Lin X, Yang H, Wang L, Li W, Diao S, Du J, Wang S, Dong enhanced the osteogenic differentiation of mesenchymal st formation of YAP/RUNX2 complex and BARX1 transcription 15;52(1):e12522–11.

28. Chen XF, Zhu DL, Yang M, Hu WX, of YDTAJ, 2018. An os

FIGURE LEGENDS

Figure 1. Promoter Capture C interactions between the *EPDR1* g
SNPs. rs1524068 (r^2=1.0, dark green), rs6975644 (r^2= 0.553249, ora
0.995712, light green) located at the '*STARD3NL*' locus (sentinel SNP
contacts between the proxy SNPs and the *EDPR1* gene promoter are
(color arcs) and located in open chromatin regions (OCRs). The 204b
region is indicate below the proxy SNPs with an arrowhead. All genes
are indicated at scale.

Figure 2. Multiplexed sequencing of CRISPR-edited hFOB1.19 ce
confirms proxy SNP deletions and reveals the efficient sgRNA pa
replicates are shown. Teal indicates wild-type sequence, pink indicate
regions, and the red bars indicate proxy SNP locations. The US3/DS3
produced the highest percentage of deletions (average 59.3%) follow
combination (average 39.6%). Variability in the CRISPR cut sites is in
error bars.

Figure 4. Western Immunoblotting reveals a decrease in EPDR1 p

CRISPR-edited hFOB1.19 cells differentiated for 7 days. Three bio
shown for each condition. **A**. Western immunoblotting detected bands
EPDR1 (25kDa) with a decrease in EPDR1 band intensities in differe
hFOB1.19 samples. Equal loading was verified with the housekeeping
(55kDa). **B**. Quantification of the upper band (U) and middle band (M)
samples shows a decrease of ~90% on average for both U and M ba
controls (empty vector).

Figure 5. Alkaline phosphatase staining (ALP) is reduced in CRIS

cells differentiated for 5 days. Three biological replicates are shown
ALP staining of plates grown under both permissive (33.5°C) and diffe
conditions. Purple color indicates alkaline phosphatase activity. **B**. Qu
staining shows an average 61% decrease in ALP staining in differenti
pValues (t-test): ***** = Empty Vector-39.5°C vs CRISPR pool-39.5°C, all
$p<0.0005$.

SUPPLEMENTARY FIGURE AND TABLE LEGENDS

Figure S1. Bright field and Texas red fluorescent microscopy of
cells at 10X magnification. Comparison of the same field under both
Red fluorescence shows a high number of mCherry positive cells in b
CRISPR pool cells for all three biological replicates. Scale bar = 200µ

Figure S2. CRISPR-cas9 primer design for the '*STARD3NL*' locus
Proxy SNPs (rs940347, rs6975644, and rs1524068) are indicated at t
region, sgRNAs are indicated by boxes, PCR primers are indicated by
sequencing primers are indicated by tailed-arrows. Diagram is to scal
locations.

Figure S3. **RNAi targeting of *EPDR1* expression decreases alkali**
(ALP) in differentiated hFOB1.19 cells. **A**. Alkaline phosphatase sta
purple staining upon activation of alkaline phosphatase during differe
staining is visible during permissive growth (33.5ºC). *EPDR1* RNAi de
5 days of differentiation (39.5ºC). **B**. Quantification shows a doubling

the two was used to calculate transduction efficiency and averaged ~8
biological replicates.

**Figure S5. PCR products generated across the '*STARD3NL*' (sen
proxy SNPs region (rs1524068, rs6975644, rs940347) from genom
of deletions in CRISPR-edited hFOB1.19 cells.** The wild type PCR
2370bp, the smallest deletion (595bp) generates a PCR product band
largest deletion (1739bp) generates a PCR product band size of 631b
combinations generate PCR products within the CRISPR deletion ran
biological replicates.

Figure S6. **RT-qPCR of CRISPR-edited hFOB1.19 derived RNA re
EPDR1 mRNA expression levels in cells grown under permissive
a dramatic decrease in *EPDR1* mRNA expression levels in** CRISP
differentiated (39.5°C) for 7 days. All three biological replicates were
then Empty Vector. pValues (t-test): # = Empty Vector vs CRISPR po
= Empty Vector-39.5°C vs CRISPR-39.5°C, all marked samples have

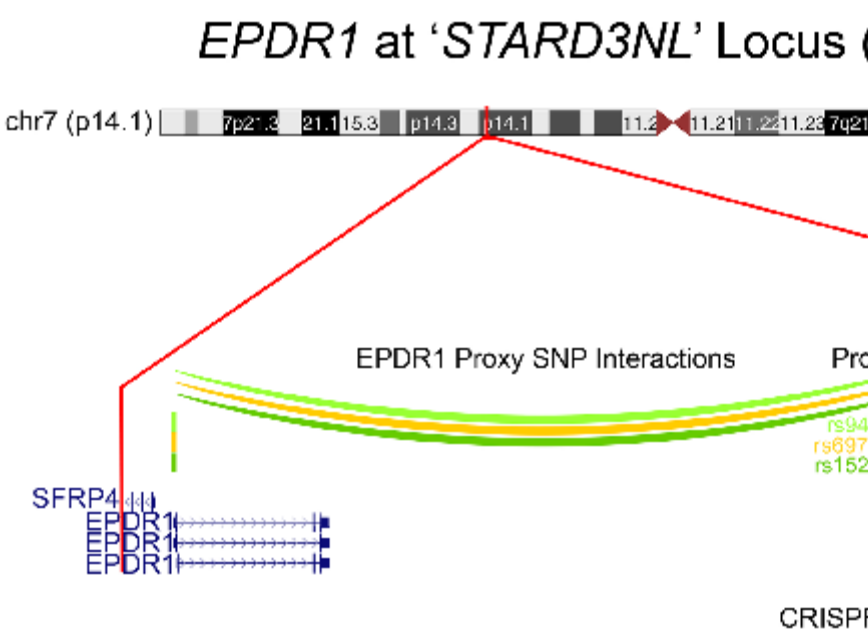

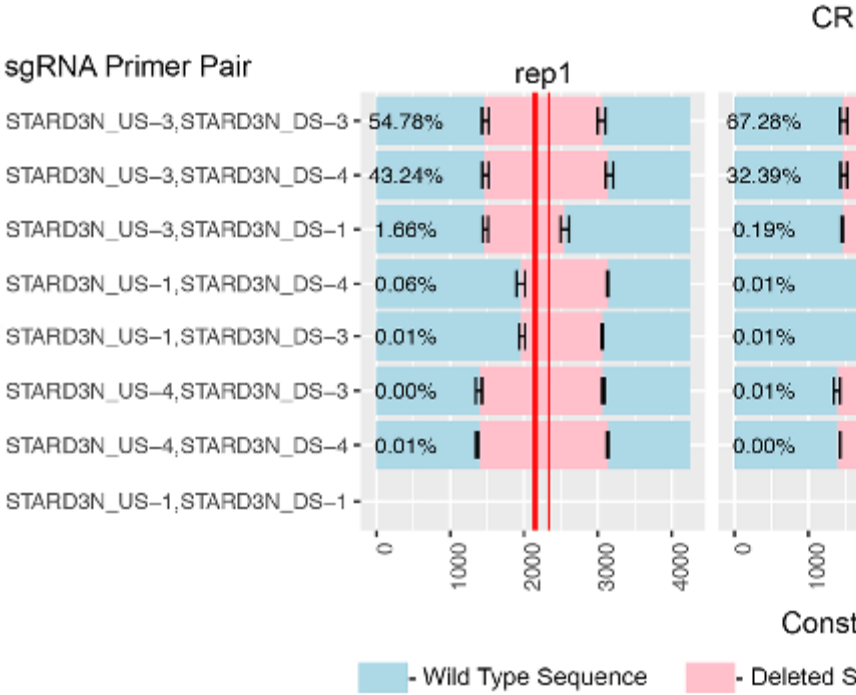

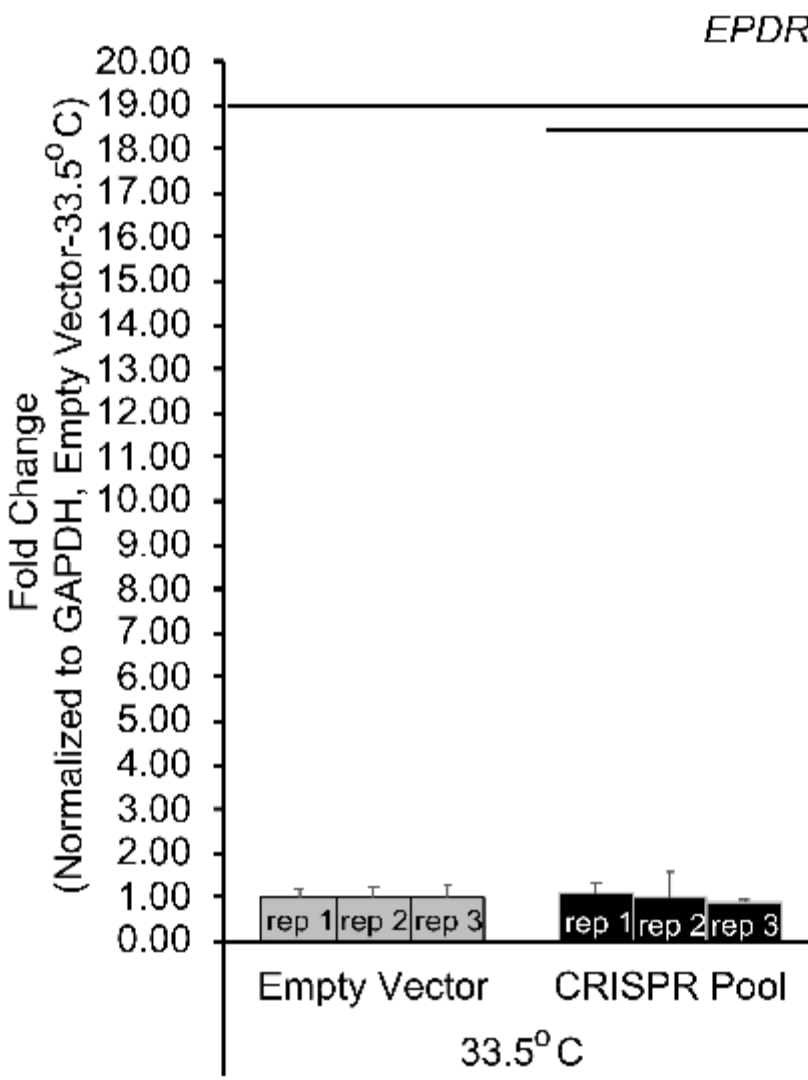

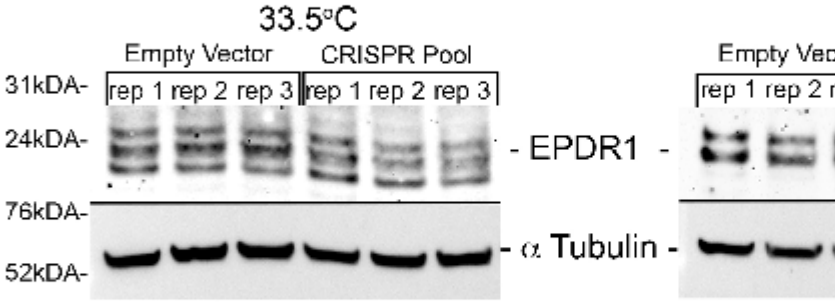

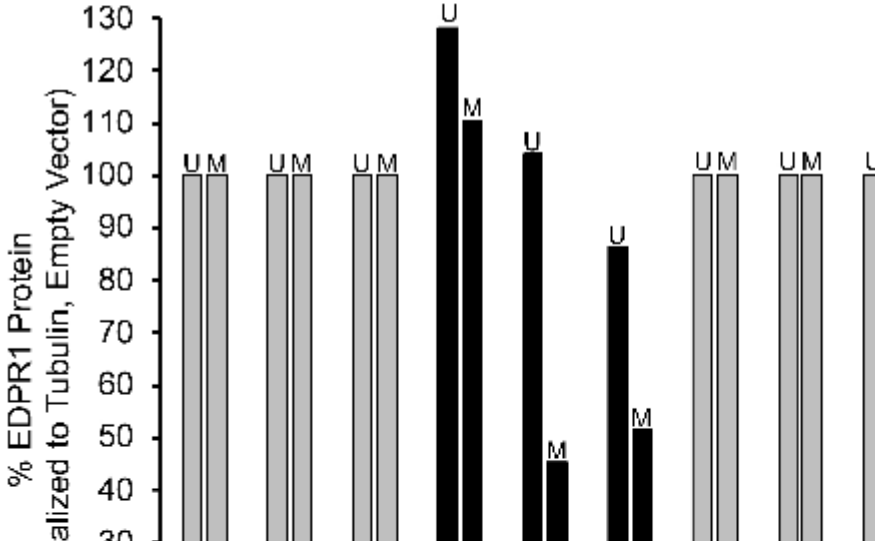

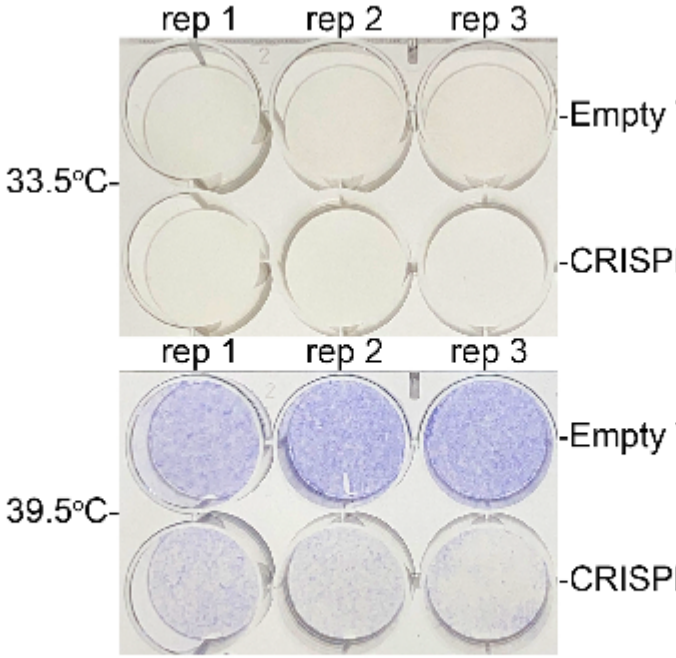

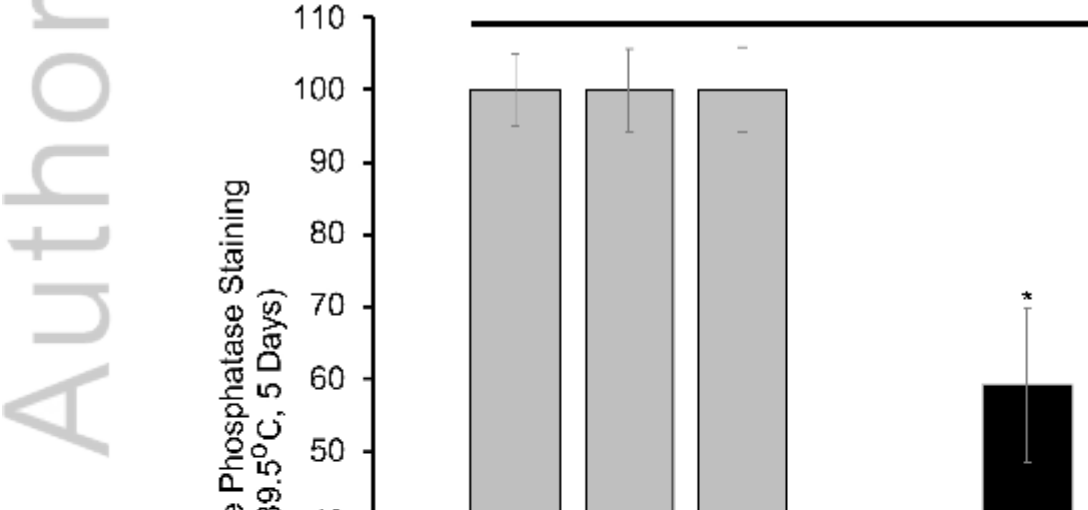

Figure 1

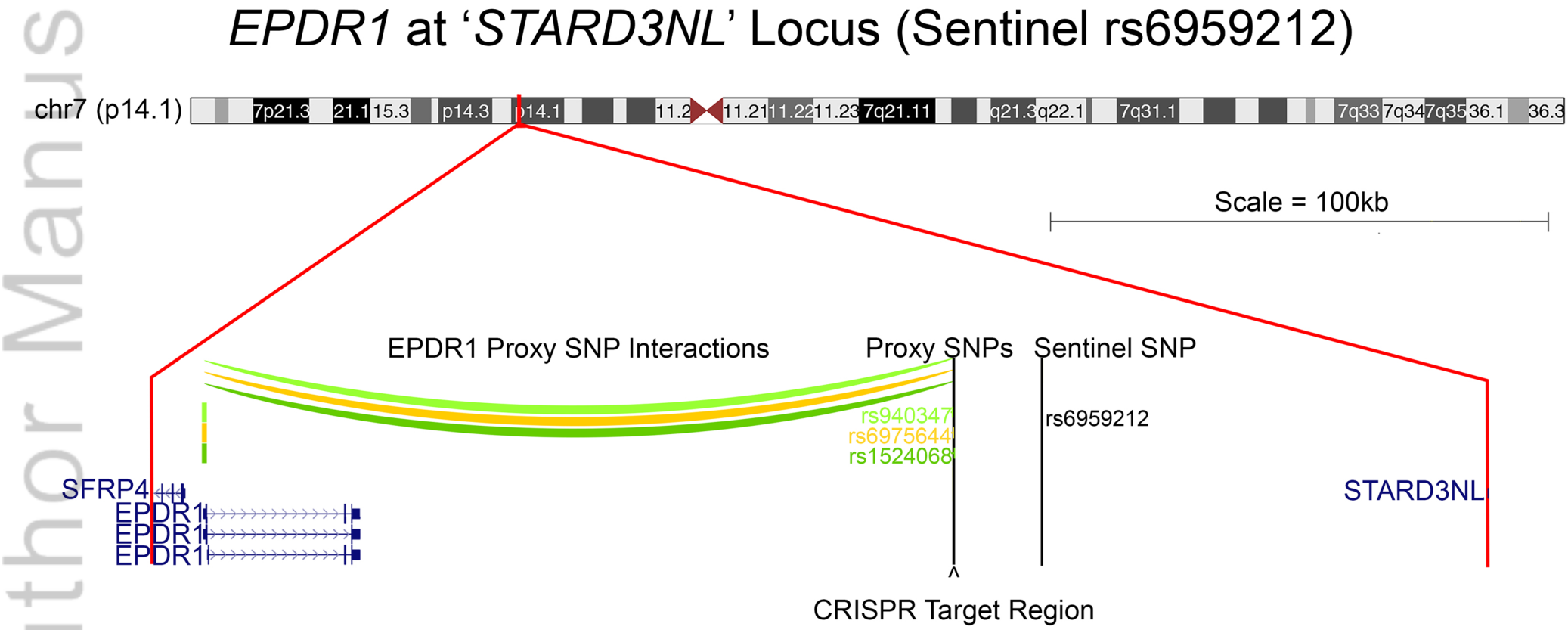

Figure 2

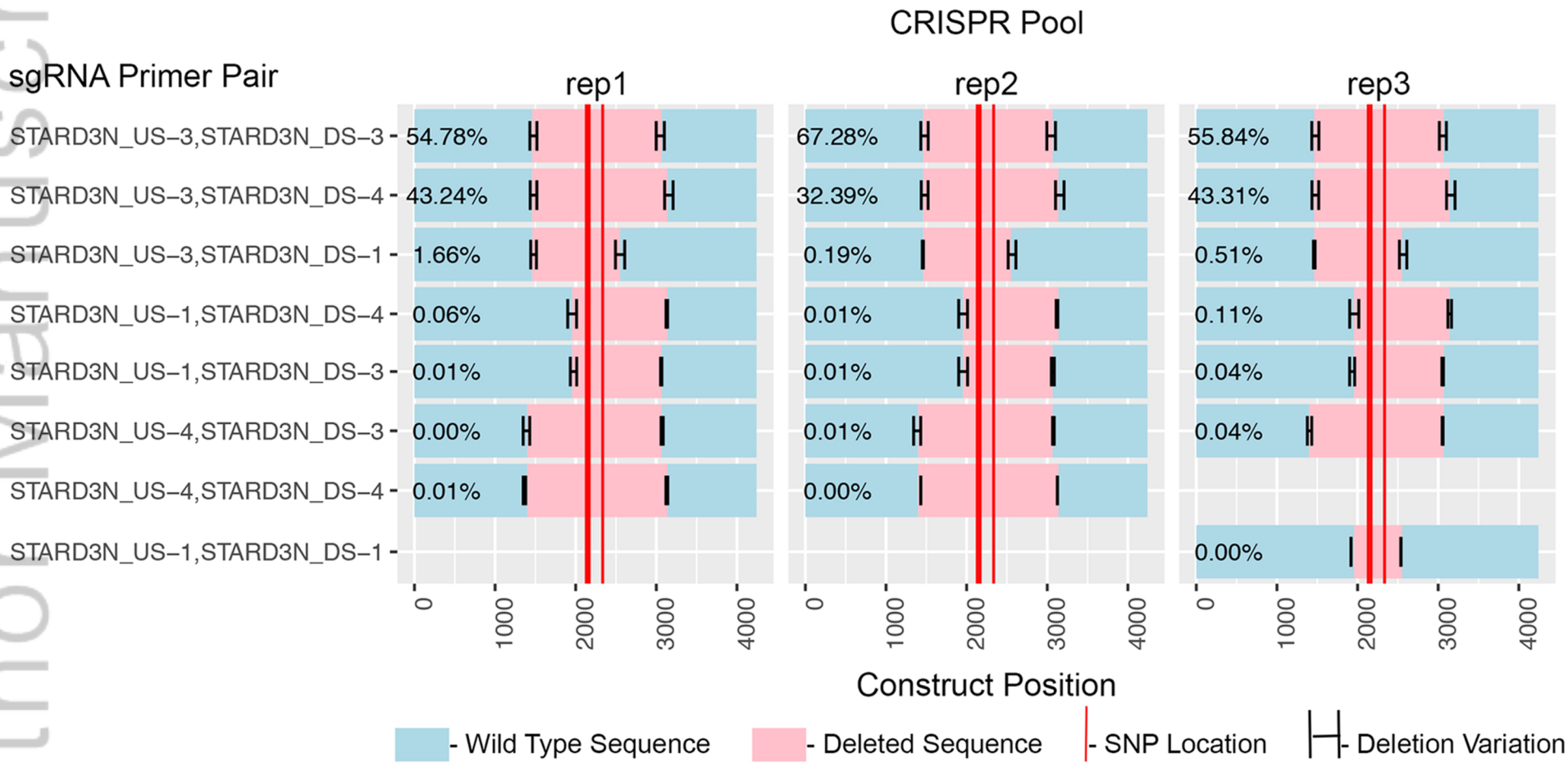

Figure 3

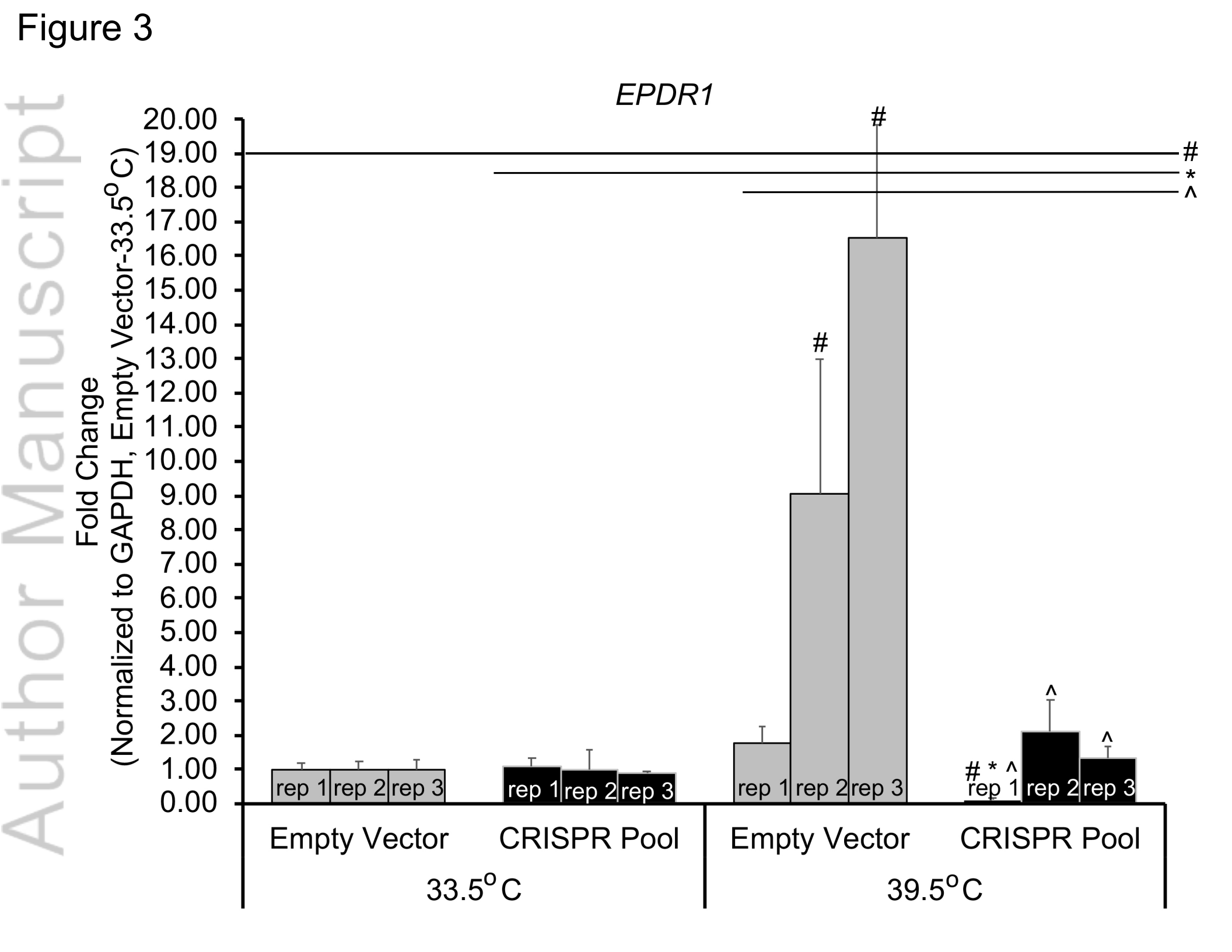

Figure 4

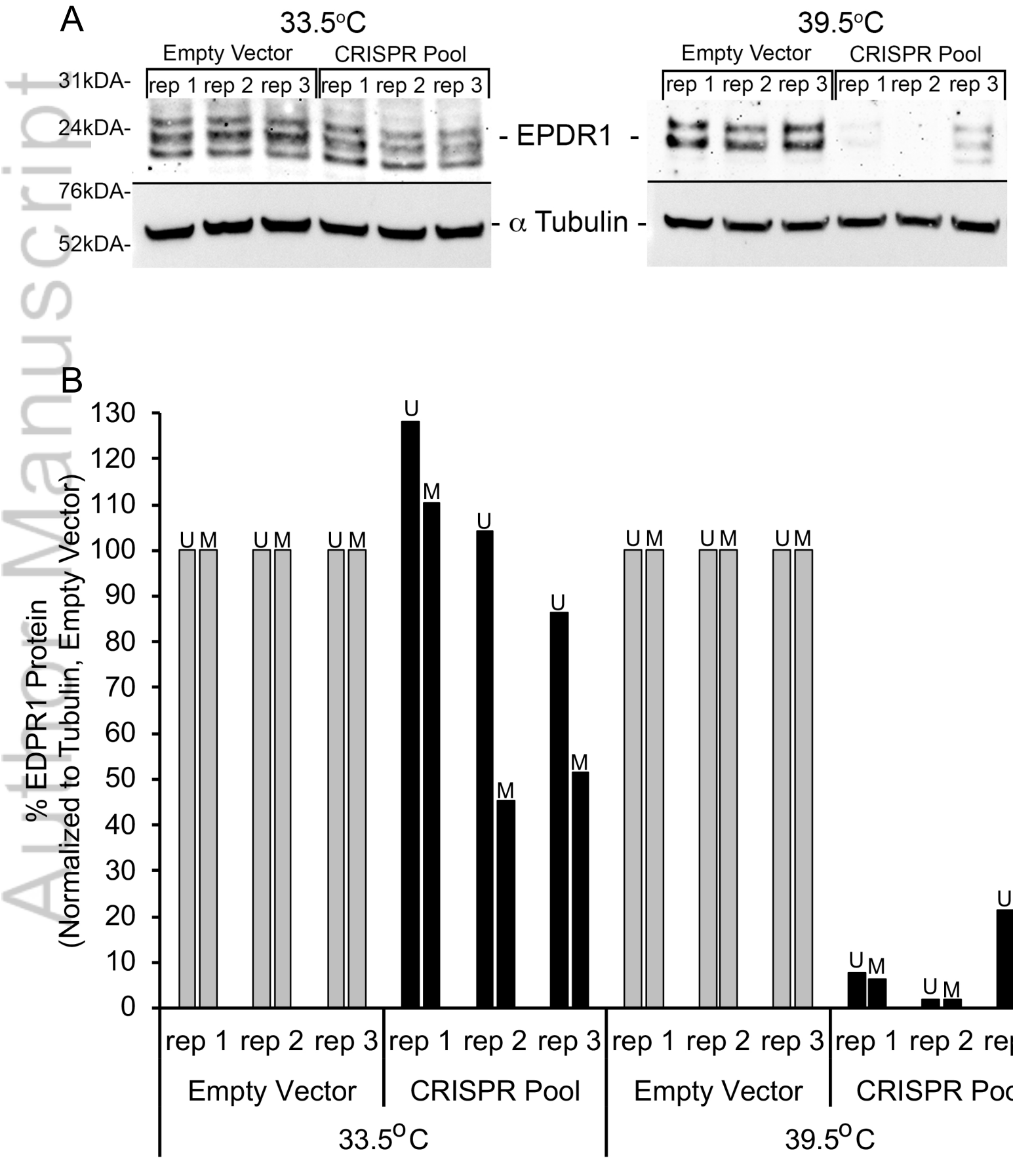

Figure 5